coatings

MDPI

Article

The Corrosion of Mn Coatings Electrodeposited from a Sulphate Bath with Te(VI) Additive and Influence of Phosphate Post-Treatment on Corrosion Resistance

Nerita Žmuidzinavičienė *, Egidijus Griškonis and Algirdas Šulčius

Department of Physical and Inorganic Chemistry, Faculty of Chemical Technology, Kaunas University of Technology, Radvilenų str. 19, 50254 Kaunas, Lithuania; egidijus.griskonis@ktu.lt (E.G.); algirdas.sulcius@ktu.lt (A.Š.)

* Correspondence: nerita.zmuidzinaviciene@ktu.lt

Abstract: Manganese coatings are excellent for the cathodic protection of steel against corrosion. Although manganese is more electrochemically active than widely used protective coatings of zinc, the exceptional resistance of manganese coatings in neutral and basic media is determined by the film of insoluble corrosion products, which forms on the surface of manganese and greatly suppresses its further corrosion. It is known that the electrodeposition process of Mn coatings from sulphate electrolytes is positively affected by some additives of chalcogenide (S, Se and Te) compounds in the electrolyte. However, a more detailed study on the corrosion properties of Mn coatings electrodeposited from sulphate bath with Te(VI) additive is lacking. In this work, the measurements of free corrosion potential and potentiodynamic polarization in a neutral NaCl solution, as well as the corrosion resistance properties of obtained Mn coatings, were evaluated in a salt spray chamber. It was obtained that the best corrosion resistance was shown by Mn coatings, electrodeposited at the cathodic current density of 15 A·dm^{-2} and at higher temperatures (60 and 80 °C). Meanwhile, the corrosion resistance of phosphated Mn coatings, obtained from a room temperature bath, increased about 5 times and reached up to 1000 h until corrosion of the steel substrate occurred.

Keywords: manganese–ammonium sulphate bath; Te additive; corrosion resistance; salt spray chamber

check for updates

Citation: Žmuidzinavičienė, N.; Griškonis, E.; Šulčius, A. The Corrosion of Mn Coatings Electrodeposited from a Sulphate Bath with Te(VI) Additive and Influence of Phosphate Post-Treatment on Corrosion Resistance. *Coatings* **2023**, *13*, 1617. https://doi.org/10.3390/coatings13091617

Academic Editor: Paweł Nowak

Received: 31 July 2023
Revised: 31 August 2023
Accepted: 12 September 2023
Published: 15 September 2023

Copyright: © 2023 by the authors. Licensee MDPI, Basel, Switzerland. This article is an open access article distributed under the terms and conditions of the Creative Commons Attribution (CC BY) license (https://creativecommons.org/licenses/by/4.0/).

1. Introduction

Manganese, an important, basic, industrial raw material with large demand, was not only used in the smelting and processing of stainless steel [1] and nonferrous alloys [2], but also widely used in electronic materials [3] and special chemicals, used in medicine, agriculture and animal husbandry departments [4]. Despite the very negative potential of Mn (E^0 = −1.18 V vs. SHE), which results in a low current efficiency, recently, electrolysis from aqueous electrolytes have become the main choice in the manganese production industry [4,5].

Manganese electrodeposition from ammonium sulphate [6] and chloride media has been well studied [7,8]. However, a sulphate bath should be chosen in order to avoid the negative impact provided by the chloride medium (Cl_2 formation and the corrosive nature of the electrolyte) [9].

It is known that electrodeposited Mn coatings obtained from aqueous solutions containing ammonium salts corrode during electrolysis [10,11]. Fast corrosion of Mn coatings and the high rate of hydrogen evolution on electrodeposited Mn coatings in ammonium sulphate/chloride electrolytes are the main disadvantageous processes during manganese electrodeposition. Additives of chalcogen compounds were used in order to avoid these disadvantages and increase the current efficiency of Mn coatings.

The electrodeposition of Mn from the sulphate bath requires selenium compound additives, such as SeO_2 or H_2SO_3 [12–16], to control the structure and morphology of

manganese coatings. The expensive and toxic SeO_2 presents hazardous effects on the environment [9,17–20], which is against the goals of green chemistry. In addition, the formation of MnSe in coatings leads to the low purity of Mn [21,22]. Therefore, sulphur dioxide SO_2 is often used in the industry, which makes it possible to obtain high purity (~99.5%) Mn coatings, but they have poor morphology [23].

From the literature review, it must be concluded that the most effective electrolytic additives used for electrodeposition of Mn are inorganic compounds, containing sulphur, selenium and tellurium. However, there is insufficient data on the Te compounds' influence on the electrodeposition of Mn coatings and their properties. Recently, the influence of some tellurium Te compound additives on the electrodeposition process of Mn coatings and their properties (structure, morphology, current efficiency, etc.) were studied [24–26].

Literature analysis on the influence of sulphur, selenium and tellurium additives on the corrosion properties of electrolytic Mn coatings is very scarce. Only one old literary source was found, where corrosion of Mn coatings electrodeposited from Se additive containing electrolytes was investigated by immersing in 3% NaCl aqueous solution and artificial groundwater, as well as by exposing them to artificial fog in a self-made corrosion chamber at 99%–100% humidity and 30 ± 1 °C temperature [27]. It was found that corrosion potential values of Mn coatings in corrosion media increase with increasing the duration of the test, and Mn coatings completely lose the protective properties with respect to the steel when oxidation of Mn occurs at temperatures above 600 °C. However, it did not provide comparative studies of Mn coatings deposited from electrolytes without S and Se additives. It is also known that during the deposition of Mn coatings from chloride electrolyte with SeO_2, an addition of sodium acetate improves the corrosion resistance of the manganese deposits [28]. However, there is no data on the influence of Te compounds on corrosion of electrodeposited Mn coatings.

Phosphate coatings are the most often used form of steel surface treatment because of their good adhesion, high-corrosion resistance, and acceptable manufacturing costs [29–31]. It was found that the manganese phosphate coatings have the highest hardness and have superior corrosion and wear resistance [32]. However, little has been published on the fundamental mechanism of the manganese hot-dip phosphatizing process widely applied for steel [33]

The aim of the present work was to investigate the influence of a tellurium(VI) additive in a sulphate bath on the corrosion properties of electrolytic Mn coatings obtained at different temperatures, and to evaluate the influence of phosphate coatings on corrosion resistance.

2. Materials and Methods

All chemicals used in this study were analytically pure (Sigma-Aldrich, St. Louis, MO, USA, and Reakhim, Moscow, Russia), and for the preparation of all solutions, twice-distilled water with resistivity ≥5 MΩ·m was used.

2.1. Electrodeposition

Mn coatings for corrosion tests were electrodeposited on mild carbon steel (ASTM A283 [34], grade A) plates of two sizes (see below). The surfaces of mild carbon steel plates before electrodeposition of Mn coatings were polished with a felt wheel by using Cr_2O_3 polishing paste, degreased with Vienna lime, thoroughly washed with tap water and distilled water, and pickled in a 2% H_2SO_4 aqueous solution. Electrodeposition of coatings was performed in a manganese–ammonium sulphate bath (MASB) of the following composition: 0.62 M $MnSO_4 \cdot 5H_2O$; 0.95 M $(NH_4)_2SO_4$ and 2.2 mM Na_2TeO_4 (pH~2.3). Since previous studies [25,26] have shown that Mn coatings of the best quality are electrodeposited from MASB at a cathodic current density of 15 A·dm^{-2} and in the temperature range from 20 to 80 °C, the corrosion properties of Mn coatings electrodeposited under analogous conditions were investigated in this work. The average thickness of all electrodeposited Mn coatings was maintained at about 10–11 μm.

2.2. Electrochemical Tests

Electrochemical studies of the corrosion of Mn coatings, electrodeposited on square mild carbon steel plates of 10 mm × 10 mm size (thickness 0.5 mm), were performed at room temperature (20 ± 1 °C) in the thermostat-deployed, three-electrode electrochemical cell, filled with naturally aerated 3% NaCl aqueous solution. A silver-silver chloride (Ag/AgCl) electrode filled with saturated aqueous KCl solution (E vs. SHE = 0.197 V) and placed in a Luggin capillary tube was used as the reference electrode (RE), and a rectangular Pt plate with a surface area of both sides ~20 cm^2 (3.0 cm × 3.3 cm size) was used as a counter electrode (CE). In all experiments, the distances between working electrode (WE)—a test sample—and the Luggin capillary, and WE and the Pt plate were kept constant and equal to ~1 mm and ~5 cm, respectively. The schematic diagram of the electrochemical cell is presented in Figure 1. The surface of the test specimen, located on the opposite side of the Luggin capillary and counter electrode (Pt plate), was isolated by coating it with epoxy resin and thus, the surface area of the test specimen was constant and equal to 1 cm^2. All potentials in this work are provided with respect to the saturated Ag/AgCl electrode. Both variations of the free corrosion potential $E_{f.corr.}$ of Mn coatings applied over time, and the potentiodynamic polarization curves in the range no less than ±160 mV around open circuit potential, were recorded by using a potentiostat–galvanostat BioLogic SP-150 (Biolgic, Seyssinet-Pariset, France) interfaced with the EC-Lab v10.39 software. Potential sweep rate of potentiodinamic polarization was 0.166 mV/s. Corrosion parameters of Mn coatings, such as the equilibrium corrosion potential $E_{corr.}$ and corrosion current density i_{corr}. were calculated according to the Tafel approximation of Butler-Volmer equation and by extrapolation of the recorded potentiodynamic polarization curves with the Tafel fit tool of the software mentioned above.

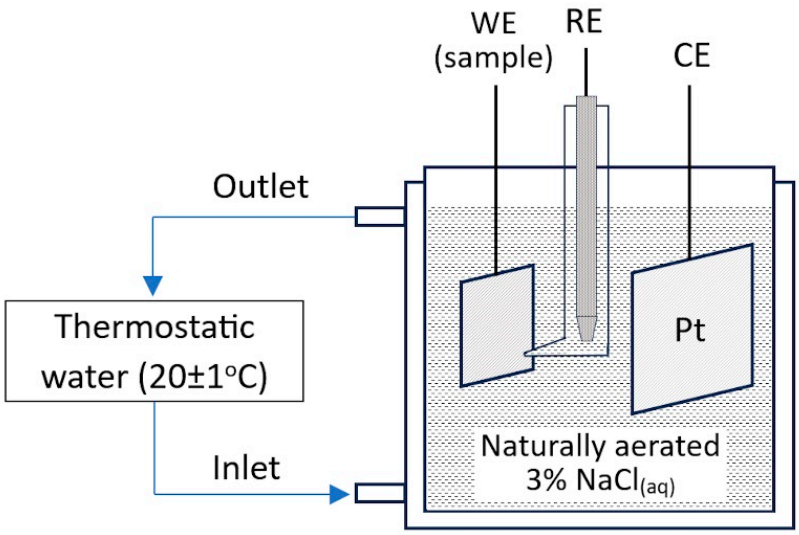

Figure 1. Schematic diagram of the electrochemical cell used in corrosion tests of Mn coatings exposed to naturally aerated 3% NaCl solution (20 ± 1 °C).

2.3. Salt Spray Test

The long-term corrosion resistance of Mn coatings, electrodeposited on rectangular mild carbon steel plates of 50 mm × 100 mm size (thickness 1.0 mm), was tested in a neutral salt spray fog atmosphere according to the standard EN ISO 9227:2022 [35]. For this certified salt spray chamber, a Q-Fog CCT 600 (Q-Lab Corporation, Westlake, OH, USA) was used. Testing in a salt spray chamber is used because it is inexpensive, quick, well standardized, and reasonably repeatable, although it does not always replicate real-world corrosive conditions and often accelerates corrosion. The salt spray fog in the chamber was generated by spraying 5% NaCl aqueous solution (pH 6.5–7.2). Temperature in the chamber was 35 ± 2 °C. The specimens' angle of inclination was 20°. The deposition

rate of salt spray on 50 cm^2 surface area of each sample was 1–2 cm^3/h. The corrosion rate of Mn coatings in salt spray fog was evaluated gravimetrically according to weight changes of samples over time. The results were calculated as the mass change average of three samples.

2.4. Phosphate Treatment

In order to improve the corrosion resistance of Mn coatings, a cold phosphating solution of this composition was used (M): $Zn(H_2PO_4)_2 \cdot 2H_2O$—0.31; $Zn(NO_3)_2 \cdot 6H_2O$—0.185; NaF—0.21; $MnCO_3$—0.087; pH 2.4–2.6; t = 20–24 °C [36]. Total acidity of the phosphating solution was 64–66 points; free acidity, 6–7 points. One point corresponds to 1 mL of 0.1 mol/L NaOH solution used to neutralize 100 mL of phosphating solution. The phosphate coating on the surface of the Mn coating were formed within 20 min and the thickness of the coating was ~0.15 g/dm^2.

2.5. Structural, Elemental and Morphological Analysis

X-ray diffraction (XRD) analysis of corrosion products formed on the surface of Mn coatings was performed by using X-ray diffractometer SmartLab (Rigaku, Tokyo, Japan) with a rotating X-ray tube with a Cu anode and Ni filter. The diffraction angle measurement range was from 10° to 70°, the measurement step 0.02°, and rotation speed of the detector $1^\circ \cdot min^{-1}$. PDF-4+ database of crystalline compounds was used for phase analysis of corrosion products.

The elemental analysis of the corrosion products formed on the surface of Mn coatings exposed in the salt spray chamber was carried out by wavelength dispersive X-ray fluorescence spectroscopy (WDXRF) using an Axios mAX spectrometer (Malvern Panalytical B.V., Eindhoven, The Netherlands) with an Rh anode X-ray tube. Chemical composition studies were performed using the benchmark quantitative elemental analysis software Omnian (Malvern Panalytical B.V., Eindhoven, The Netherlands). The samples for XRD and WDXRF were prepared by grinding the corrosion products scraped from the surface of Mn coatings and forming 20 mm diameter tablets.

The investigation of surface morphology of Mn electrodeposits was performed using a FEI Qanta 200 FEG (Hillsboro, OR, USA) scanning electron microscope (SEM).

3. Results and Discussion

3.1. Corrosion of Mn Coatings in Naturally Aerated 3% NaCl Aqueous Solution

First of all, we performed long-term measurement of free corrosion potential ($E_{f.corr.}$) in naturally aerated 3% NaCl aqueous solution of mild carbon steel substrate via Mn electrodeposits. It was observed (Figure 2) that the values of $E_{f.corr.}$ for mild carbon steel substrate decreased the most, i.e., from −470 to −690 mV, during the first 24 h, and then, a uniform drop to −720 mV was observed for the rest of the observational period (up to 240 h). It shows that the steel substrate corrodes without passivation. Meanwhile, the values of free corrosion potential of Mn coatings, electrodeposited from MASB with 2.2 mM Te(VI) additive ata cathodic current density of 15 A dm^{-2} and in a temperature range of 20–80 °C, increase over time, and this could be associated with manganese's tendency to passivate.

The fastest increase of the free corrosion potential from −1250 mV to −1100 mV was observed in the first 24 h for Mn coatings, obtained from MASB at room temperature (20 °C). After the first 24 h, the free corrosion potential stabilised and slowly increased up to −1050 mV during the remaining time of the experiment (up to 240 h). The free corrosion potential of Mn coatings electrodeposited from MASB at 40 °C stabilised after 48 h and increased slightly from −1160 mV to −1120 mV during the remaining time of the experiment (up to 240 h). The free corrosion potential of Mn coatings electrodeposited from MASB at 60 °C increased linearly from −1250 mV to −1115 mV over the entire experiment period.

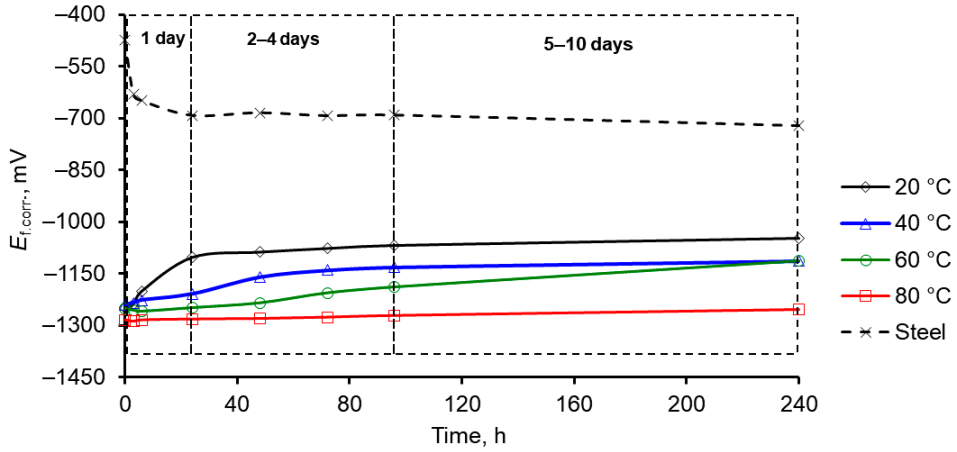

Figure 2. Change of the free corrosion potential $E_{f.corr.}$ over time of mild carbon steel substrate and Mn coatings in naturally aerated 3% NaCl solution at 20 ± 1 °C temperature. Mn coatings were electrodeposited on steel substrate at a cathodic current density of 15 A·dm^{-2} and various temperatures (20, 40, 60 and 80 °C) of MASB, containing 2.2 mM of Te(VI) additive.

Finally, the free corrosion potential of Mn coatings electrodeposited from MASB at 80 °C stayed relatively stable, while varying in a narrow range from −1280 to −1290 mV during the first 24 h, and then slowly increased up to −1250 mV during the remaining observation time. It is important to note that these coatings had the lowest free corrosion potential when compared to the other Mn electrodeposits obtained at lower temperatures.

During the corrosion of Mn coatings, in naturally aerated 3% NaCl solution, the formation of dark-brown coloured precipitate was observed. This precipitate most likely consisted of Mn hydroxide and/or Mn basic salts, and resembled a light-brown precipitate (presumably Fe(III) hydroxide and/or Fe(III) basic salts) formed during the corrosion of mild carbon steel.

In order to analyse the progress of corrosion of Mn coatings in naturally aerated 3% NaCl aqueous solution, the potentiodynamic polarisation curves were recorded at different times (after 1 h, 24 h, 72 h, and 240 h) after immersing the samples into the corrosive medium (Figure 3).

After Tafel approximation of these curves, the values of Tafel constants for anodic and cathodic processes (β_a and β_c, respectively) were determined. By applying approximations of Butler–Volmer equation when the electrode potential was $E >> E_{corr.}$ and $E << E_{corr.}$, the corrosion equilibrium potential E_{corr} and current density i_{corr} were calculated (Table 1). The values of equilibrium corrosion potential of Mn coatings calculated by using this method (Table 1) accurately correlate with the experimentally obtained values of free corrosion potential and their changes over time (Figure 1). It should be noted that, the higher the temperature during the electrodeposition of Mn coating from MASB, the lower the corrosion potential values are in naturally aerated 3% NaCl solution, i.e., the coatings are more electronegative.

The calculated values of corrosion current density, which are directly proportional to the corrosion rate and their change over time (Figure 4), showed that Mn coatings electrodeposited from MASB with 2.20 mM Te(VI) additive at a cathodic current density of 15 A·dm^{-2} and at lower temperatures (20 °C and 40 °C) had the fastest corrosion rate during the first hour after immersing into the corrosive medium. However, after one day, the corrosion current density and corrosion rate of these Mn electrodeposits decreased up to four and two times, respectively, whereas after 3–10 days these coatings corroded even 2.5–3 times slower than 1 h after immersion into the corrosive medium.

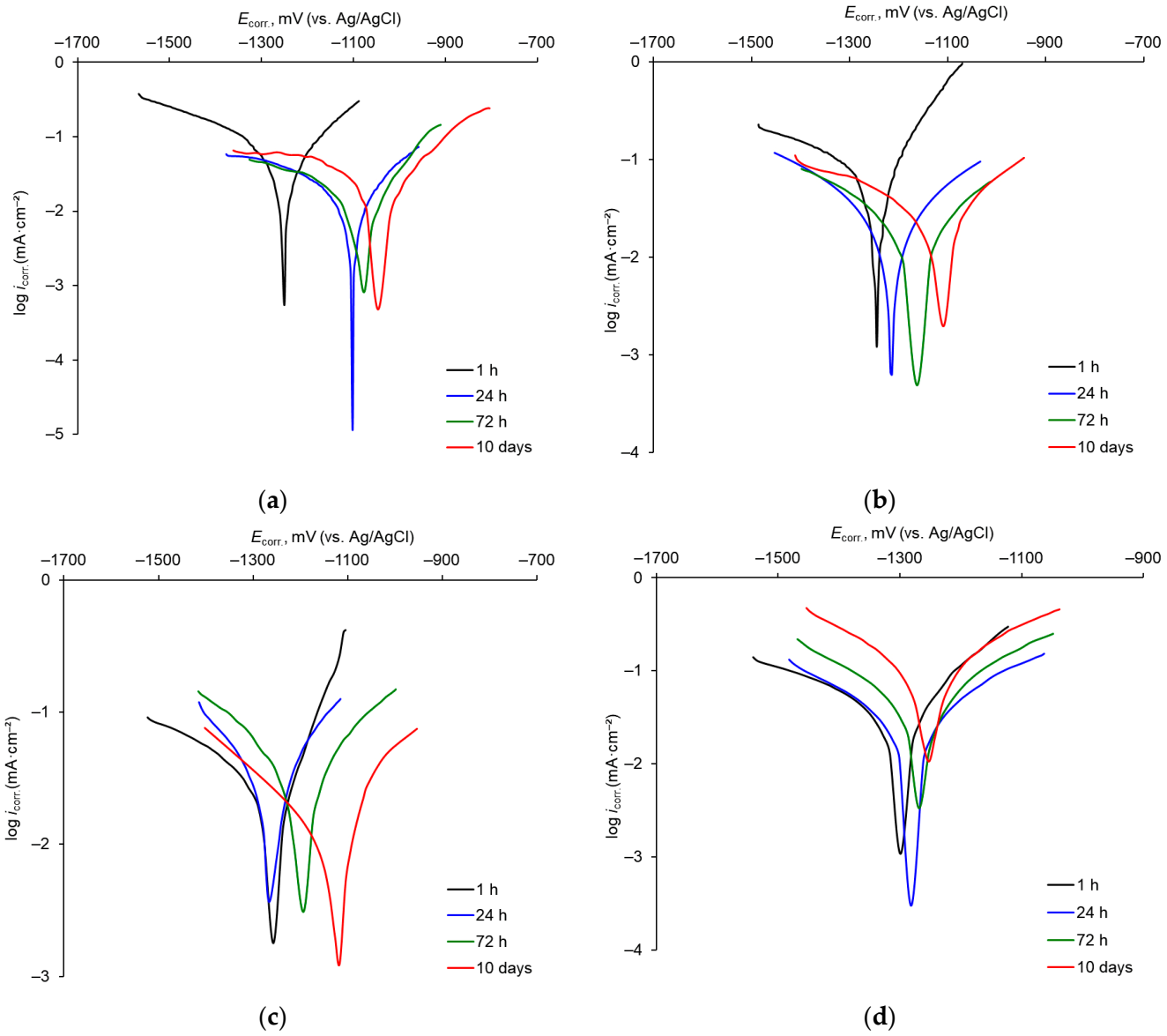

Figure 3. Potentiodynamic polarization curves of Mn coatings recorded after different periods of corrosion in naturally aerated 3% NaCl solution at 20 ± 1 °C temperature. Mn coatings were electrodeposited on steel substrate at a cathodic current density of 15 A·dm^{-2} and various temperatures of MASB, containing 2.2 mM of Te(VI) additive: (**a**) 20 °C; (**b**) 40 °C; (**c**) 60 °C; (**d**) 80 °C.

This can be explained by the formation of a corrosion product film, which possesses good protective properties and provides passivation of the Mn coatings. Meanwhile, Mn coatings, electrodeposited from MASB with 2.2 mM Te(VI) additive at 60 °C and a cathodic current density of 15 A·dm^{-2}, corroded the slowest at 1 h after the initial immersion moment. However, after one day, their corrosion rate increased, as the value of $i_{corr.}$ Nearly doubled. After 3–10 days, the $i_{corr.}$ Of these Mn coatings suddenly decreased nearly to the initial level, and the corrosion rate was close to that of the Mn coatings electrodeposited from MASB at 20 °C and 40 °C.

Table 1. Corrosion parameters of Mn coatings, electrodeposited on steel substrate at a cathodic current density of 15 A·dm^{-2} and various temperatures of MASB, containing 2.2 mM of Te(VI) additive. Corrosion parameters were determined by Tafel fitting of potentiodynamic polarization curves recorded after different exposition periods in naturally aerated 3% NaCl solution (20 ± 1 °C).

Temperature of MASB, °C	Corrosion Time, h	$E_{corr.}$, V (vs. Ag/AgCl)	$i_{corr.}$, μA·cm^{-2}	$-\beta_c$, mV·dec^{-1}	β_a, mV·dec^{-1}
20	1	−1251	93.4	66.7	37.5
	24	−1104	22.6	96.2	37.1
	72	−1082	14.1	60.6	23.6
	240	−1048	41.1	233.2	44.1
40	1	−1249	97.7	99.8	24.8
	24	−1215	52.4	81.8	70.4
	72	−1169	39.6	96.5	72.9
	240	−1114	31.5	122.8	38.8
60	1	−1257	37.9	68.4	18.4
	24	−1267	79.8	126.1	84.8
	72	−1193	35.9	125.0	96.8
	240	−1117	10.4	54.1	20.1
80	1	−1288	64.2	94.2	34.4
	24	−1282	73.6	89.9	73.8
	72	−1269	114.8	87.4	70.1
	240	−1253	258.8	83.1	84.5

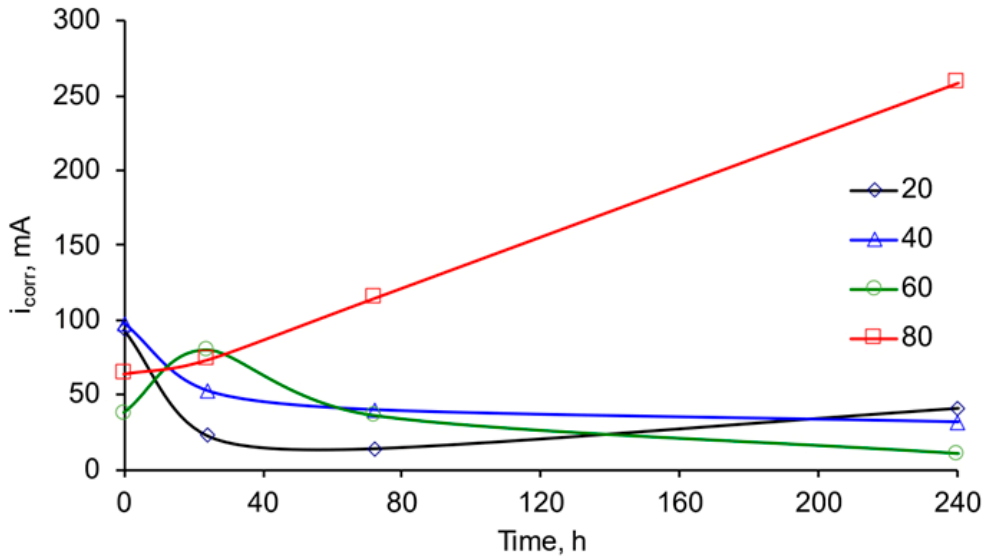

Figure 4. Change in corrosion current density $i_{corr.}$ Of Mn coatings in naturally aerated 3% aqueous NaCl solution over time. Mn coatings were electrodeposited on steel substrate from the MASB with 2.20 mM Te (VI) additive at a cathodic current density of 15 A·dm^{-2} and different temperatures (20, 40, 60 and 80 °C).

The linear increase of $i_{corr.}$ Values, and thus the corrosion rate over time, is characteristic to the Mn coatings electrodeposited from MASB at 80 °C. The corrosion of such coatings intensified almost twice within 1–3 days, and after 10 days the corrosion current density was four times higher than the one measured 1 h after immersion into the corrosive medium. Such observation could be explained by a greater corrosive activity of the Mn coating itself, which could be caused by possible surface defects and the formation of the poorly adhering, porous film of corrosion products on the surface of these coatings. Overall, all the differences in corrosion rates of Mn coatings electrodeposited from MASB of different temperatures is most probably caused by structural and morphological fea-

tures of the coatings, as well as the variation of concentrations of Te incorporated into Mn electrodeposits [25]. Since in all cases examined, the Tafel constant value of cathodic corrosion process was greater than the one of anodic corrosion process ($\beta_c > \beta_a$), based on the literature data [37], it may be assumed that Mn corrosion was limited by the cathodic process, i.e., in formation of hydroxide ions:

$$O_{2(g)} + 2H_2O_{(l)} + 4e^- \rightarrow 4OH^-{}_{(aq)}$$

An anodic process that did not limit the corrosion kinetics was oxidation of manganese:

$$Mn_{(s)} \rightarrow Mn^{2+}{}_{(aq)} + 2e^-$$

3.2. Corrosion of Mn Coatings in a Salt Spray Chamber

In order to accurately determine the behaviour of electrolytic Mn coatings for the long-term protection of a steel base, they were tested in a salt spray fog atmosphere. Corrosion resistance of Mn coatings was evaluated gravimetrically, according to the mass changes of the coatings per unit area over time. The tests in the salt spray chamber showed that during the initial stages of corrosion (within first 24 h), the mass of Mn coatings did not decrease significantly (Figure 5), which is most likely due to the formation of more soluble Mn corrosion products, one of which is likely to be Mn(II) chloride. However, as the corrosion progressed, poorly soluble and insoluble corrosion products accumulated on the Mn coatings, and then the mass of the samples increased (Figure 5).

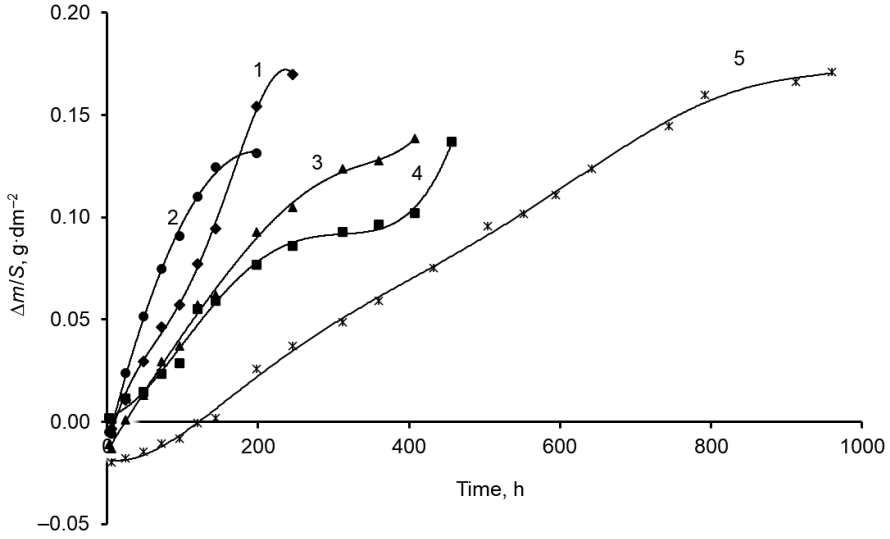

Figure 5. Mass change per area unit for the Mn coatings in the salt spray chamber over time. Mn coatings were electrodeposited on steel substrate from MASB with Te(VI) additive at a cathodic current density of 15 A·dm^{-2} and different temperatures: 1—20 °C; 2—40 °C; 3—60 °C; 4—80 °C; 5—20 °C + phosphated.

The mass of Mn coating electrodeposited from MASB of lower temperatures (20–40 °C) increased the fastest in the salt spray chamber. These coatings had fully corroded after 8–10 days (192–240 h), when the signs of corrosion of the steel base were noticeable on the surface (Figure 2). Meanwhile, the mass of Mn coatings electrodeposited from MASB of higher temperatures (60–80 °C) increased slower. These types of coatings were able to protect the steel base for twice as long. The corrosion of steel bases coated with these coatings occurred only after 17–19 days (408–456 h) in the salt spray chamber. The indicators of corrosion, i.e., formation of various coloured compounds from Mn coating and steel, on the surface of Mn electrodeposits after testing in the salt spray chamber, and time until their occurrence, are presented in Table 2.

Table 2. Time of the appearance of corrosion products on the surface of Mn coatings and changes in appearance during exposure time in the salt spray chamber. Mn coatings were electrodeposited on steel substrate from MASB with Te(VI) additive at a cathodic current density of 15 A·dm^{-2} and different temperatures. Some samples were additionally phosphated.

Temperature of MASB, °C	The Appearance of:					
	Individual Dark Brown or Black Dots	Bluish Spots	Dark Brown Spots	White Spots	Orange Spots	Corrosion of Steel Substrate
20	6 h	6 h	72 h	66 h	72 h	240 h
40	3 h	6 h	36 h	126 h	84 h	192 h
60	12 h	24 h	42 h	48 h	108 h	after 408 h, corroded coating separates from the steel substrate
80	12 h	42 h	42 h	42 h	78 h	after 456 h, only at the corners of the samples
20+ phosphated	24 h	312 h	192 h	264 h	-	960 h

Typical SEM views of the surface of Mn coatings, electrodeposited from different MASB temperatures with 2.2 mM Te(VI) additive at a cathodic current density of 15 A·dm^{-2}, and exposed in the salt spray chamber for a long time (7 days), are presented in Figure 6. As shown, as the MASB temperature increases, a more compact and uniform layer of corrosion products forms on the surface of the Mn electrodeposits under the attack of salt spray. This may be related to the tendency of quality improvement of Mn coatings when increasing MASB temperature.

Since the electrodeposition of Mn coatings from the room temperature (20 °C) MASB is both technologically and energy-wise more favourable (there is no need to heat the electrolyte and as a result, its intensive evaporation is also avoided, the electrolyte composition remains more stable, etc.), these coatings were selected for additional phosphating to increase their corrosion resistance. It was noticed that after the application of an additional phosphating procedure for Mn coatings (Figure 7a), a continuous macrocrystalline film of insoluble phosphates formed on their surface (Figure 7b), and this significantly increased the longevity of such complex coatings (Mn + phosphate film). The mass of phosphated Mn coatings increased the slowest during corrosion in the salt spray chamber, and indications of the corrosion of the steel base were noticed only after 38 days (912 h). Higher resistance to corrosion in the salt spray chamber of phosphated Mn coatings can be explained by the fast passivation of the Mn coating surface by the insoluble phosphate film. SEM analysis showed that even after performing such a long corrosion procedure, the surface of the steel substrate remained covered in phosphated Mn coating and a layer of insoluble corrosion products (Figure 7c,d).

The chemical composition (chemical elements and their mass fraction concentration) of non-phosphated and phosphated Mn coatings electrodeposited from MASB of room temperature was determined by performing WDXRF analysis (Table 3). The results of the analysis showed that the main elements in corrosion products of non-phosphated Mn electrodeposits were manganese (most probable in the form of Mn(II) oxide) and iron—the main element of the steel base (most probable in the form of Fe(III) oxide). On the other hand, the main element in the corrosion product of phosphated Mn coating was exclusively manganese (also in the form of Mn(II) oxide), and the concentration of iron was almost 10 times smaller than in the corrosion products of non-phosphated Mn coatings. Phosphorus is a characteristic of phosphated Mn coatings, and most likely was in a form of poorly soluble Mn(II) phosphate. It should be noted that in the corrosion products

of phosphated Mn coatings, there were no traces of Zn, which is the main metal in the phosphatation solution.

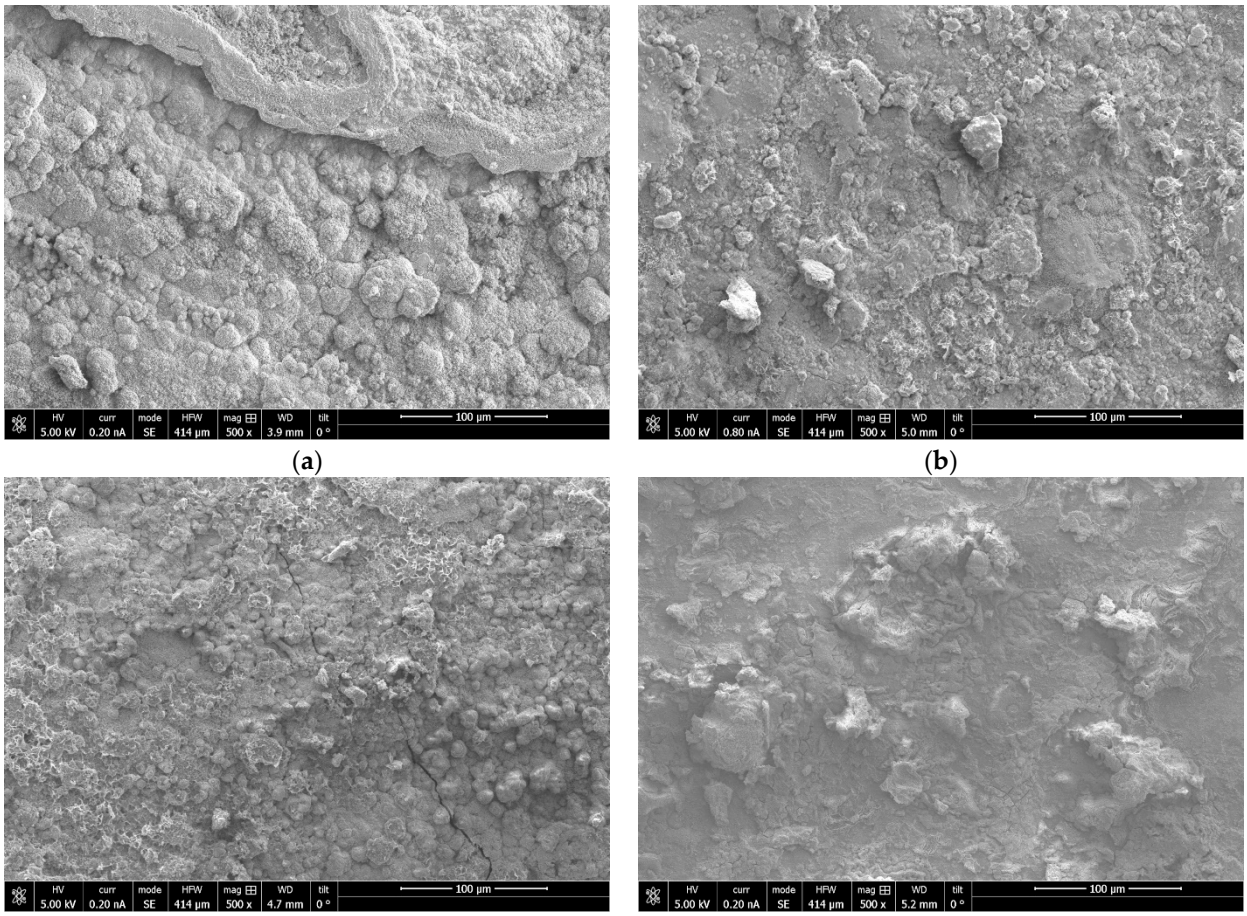

Figure 6. SEM images of Mn coatings after corrosion in the salt spray chamber. Mn coatings were electrodeposited on steel substrate from MASB with Te(VI) additive at a cathodic current density of 15 A·dm^{-2} and different temperatures: (**a**) 20 °C; (**b**) 40 °C; (**c**) 60 °C; (**d**) 80 °C.

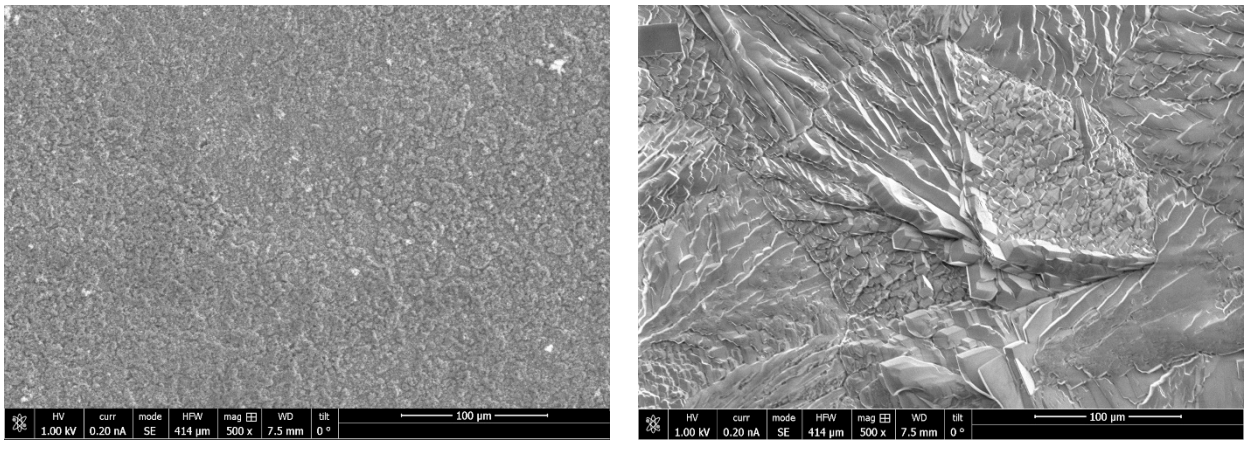

Figure 7. *Cont.*

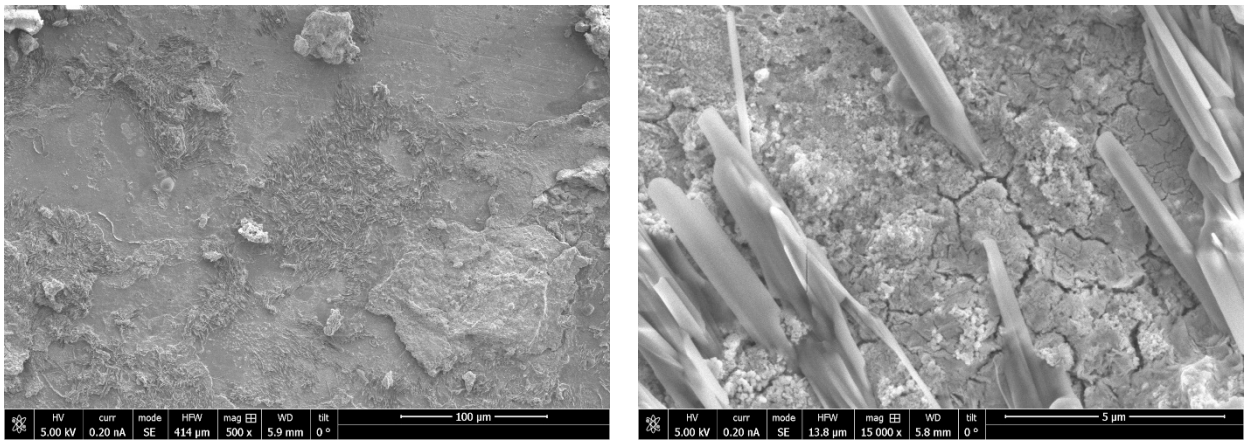

(**c**) (**d**)

Figure 7. SEM images of Mn coatings electrodeposited on steel substrate from MASB at a cathodic current density of 15 A·dm^{-2} and 20 °C temperature: (**a**)—non-phosphated; (**b**)—phosphated, before exposure in the salt spray chamber, (**c**,**d**)—phosphated, after removal from the salt spray chamber. Magnification: (**a**–**c**)—×500; (**d**)—×15,000.

Table 3. WDXRF analysis data of corrosion products formed on the surface of non-phosphated and phosphated Mn coatings, exposed in salt spray chamber up to corrosion of steel substrate. Mn coatings were electrodeposited from MASB with Te(VI) additive at a cathodic current density of 15 A·dm^{-2} and 20 °C temperature.

Temperature of MASB, °C	Element, at. %
20	O—25.58 Na—1.13 Si—0.09 S—0.02 Cl—0.91 Mn—49.16 Fe—22.75 Te—0.35
20 + phosphated	O—30.8 Na—0.00 Si—0.15 S—0.10 Cl—0.76 Mn—63.33 Fe—2.04 P—3.03 Te—0.42

After performing XRD analysis of corrosion products of Mn coatings electrodeposited from MASB of various temperatures and corrosion products of additionally phosphated Mn coatings, it was determined that due to the effects of the salt spray chamber, various oxidic Mn(II) and Mn(III) compounds, such as MnO_2, $MnO{\cdot}MnOOH$, $MnO{\cdot}Mn_2O_4$, and $MnCO_3$ were formed on the surface of the coatings (Figure 8). It was noted that the characteristic peaks of $FeO{\cdot}Fe_2O_3$ in the XRD pattern for corrosion products of phosphated Mn coatings were significantly less intense than those of corrosion products of non-phosphated Mn coatings. These XRD pattern results add on to the data of WDXRF analysis and make them more accurate.

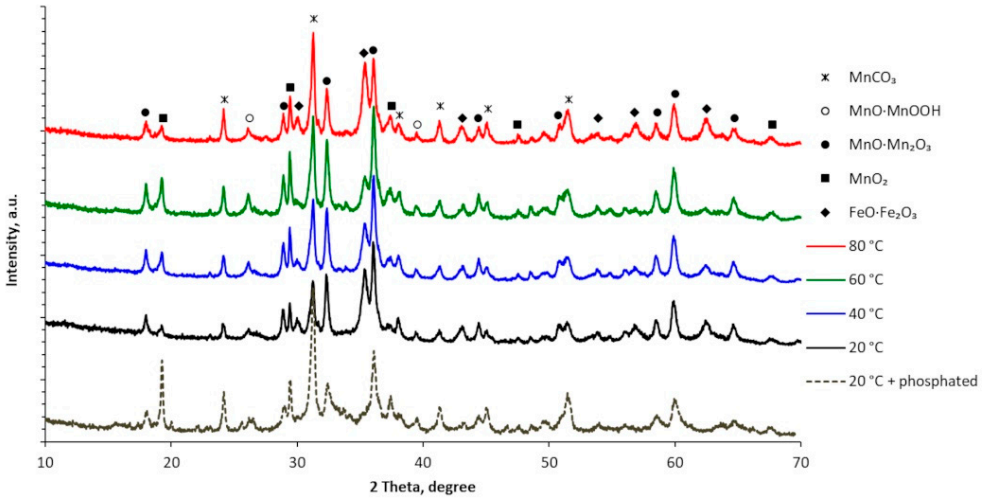

Figure 8. XRD patterns of corrosion products formed on the surface of non-phosphated and phosphated Mn coatings, exposed in salt spray chamber up to corrosion of steel substrate. Mn coatings were electrodeposited from MASB with Te(VI) additive at a cathodic current density of 15 A·dm^{-2} and different temperatures.

4. Conclusions

Based on free corrosion potential and corrosion current measurements of Mn coatings in a naturally aerated 3% NaCl aqueous solution, and data of the experiments in the salt spray chamber, the following was found:

- The most resistant to corrosion were Mn coatings, electrodeposited from higher temperature (60–80 °C) MASB at 15 A·dm^{-2} cathodic current density and containing incorporated Te (about 1.1–1.4 wt. %). The increased corrosion resistance of Mn coatings, electrodeposited at higher temperatures, could be associated with the changes in their structure from the mixture of α-Mn and β-Mn phases to α-Mn phase and a two-fold decrease in crystallite sizes of Mn coatings [25], and all this ultimately leads to an overall improvement in the quality of Mn coatings.
- The corrosion resistance of Mn coatings can be significantly increased by additionally coating them with a phosphate film. The corrosion resistance of phosphated Mn coatings, electrodeposited from room temperature (20 °C) MASB, increases by a factor of about five times and reaches 1000 h before corrosion of the steel substrate occurs.

Author Contributions: Conceptualization, A.Š.; methodology, N.Ž. and E.G.; validation, N.Ž. and E.G.; investigation, N.Ž.; resources, N.Ž.; writing—original draft preparation, N.Ž.; writing—review and editing, E.G. and A.Š.; visualization, N.Ž. and E.G.; supervision, A.Š. All authors have read and agreed to the published version of the manuscript.

Funding: This research received no external funding.

Institutional Review Board Statement: Not applicable.

Informed Consent Statement: Not applicable.

Data Availability Statement: Not applicable.

Conflicts of Interest: The authors declare no conflict of interest.

References

1. Yamaguchi, T.; Nagano, H.; Murai, R.; Sugimori, H.; Sekiguchi, C.; Sumi, I. Development of Mn recovery process from waste dry cell batteries. *J. Mater. Cycles Waste Manag.* **2018**, *20*, 1909–1917. [CrossRef]
2. Sun, Y.; Tian, X.K.; He, B.B.; Yang, C.; Pi, Z.; Wang, Y.; Zhang, S. Studies of the reduction mechanism of selenium dioxide and its impact on the microstructure of manganese electrodeposit. *Electrochim. Acta* **2011**, *56*, 8305–8310. [CrossRef]
3. Lu, J.; Dreisinger, D.; Glück, T. Manganese electrodeposition—A literature review. *Hydrometallurgy* **2014**, *141*, 105–116. [CrossRef]

4. Xie, Z.; Liu, Z.; Zhang, X.; Yang, L.; Chang, J.; Tao, C. Electrochemical oscillation on anode regulated by sodium oleate in electrolytic metal manganese. *J. Electroanal. Chem.* **2019**, *845*, 13–21. [CrossRef]
5. Wei, Q.F.; Ren, X.L.; Du, J.; Wei, S.J.; Hu, S.R. Study of the electrodeposition ditions of metallic manganese in an electrolytic membrane reactor. *Miner. Eng.* **2010**, *23*, 578–586. [CrossRef]
6. Fernández-Barcia, M.; Hoffmann, V.; Oswald, S.; Giebeler, L.; Wolff, U.; Uhlemann, M.; Gebert, A. Electrodeposition of manganese layers from sustainable sulfate based electrolytes. *Surf. Coat. Technol.* **2018**, *334*, 261–268. [CrossRef]
7. Caoa, X.; Dreisinger, D.B.; Lua, J.; Belangerb, F. Electrorefining of high purity manganese. *Hydrometallurgy* **2017**, *171*, 412–421. [CrossRef]
8. Diaz-Arista, P.; Trejo, G. Electrodeposition and characterization of manganese coatings obtained from acidic chloride bath containing ammonium thiocyanate as an additive. *Surf. Coat. Technol.* **2006**, *201*, 3359–3367. [CrossRef]
9. Padhy, S.K.; Patnaik, P.; Thipathy, B.; Bhattacharya, I. Microstructural aspects of manganese metal during its electrodeposition from sulphate solutions in the presence of quaternary amines. *Mater. Sci. Eng.* **2015**, *193*, 83–90. [CrossRef]
10. Gonsalves, M.; Pletcher, P. A study of the electrodeposition of manganese from aqueous chloride electrolytes. *J. Electroanal. Chem.* **1990**, *285*, 185–193. [CrossRef]
11. Mulin, E.V.; Kistosturov, N.I.; Tarasenkova, V.P.; Solovjov, V.A. Influence of catholite circulation and ammonium chloride on manganese current efficiency during electrolysis. *Russ. J. Electrochem.* **1984**, *20*, 1429–1434.
12. Yang, F.; Jiang, L.; Yu, X.; Lai, Y.; Li, J. The effects of SeO_2 additive on Mn electrodeposition on Al substrate in $MnSO_4$-$(NH_4)_2SO_4$-H_2O solution. *Hydrometallurgy* **2020**, *192*, 105285. [CrossRef]
13. Xu, F.; Dan, Z.; Zhao, W.; Han, G.; Sun, Z.; Xiao, K.; Jiang, L.; Duan, N. Electrochemical analysis of manganese electrodeposition and hydrogen evolution from pure aqueous sulfate electrolytes with addition of SeO_2. *J. Electroanal. Chem.* **2015**, *741*, 149–156. [CrossRef]
14. Rojas-Montes, J.C.; Pérez-Garibay, R.; Uribe-Salas, A.; Bello-Teodoro, S. Selenium reaction mechanism in manganese electrodeposition process. *J. Electroanal. Chem.* **2017**, *803*, 65–71. [CrossRef]
15. P´erez-Garibay, R.; Rojas-Montes, J.; Bello-Teodoro, S.; Flores-Álvarez, J.M. Effect of SeO_2 on the morphology of electrodeposited manganese. *J. Appl. Electrochem.* **2020**, *50*, 1291–1299. [CrossRef]
16. Xie, Z.; Liu, Z.; Tao, C.; Li, C.; Chang, J. Production of electrolytic manganese metal using a new hyperchaotic circuit system. *J. Mater. Res. Technol.* **2022**, *18*, 4804–4815. [CrossRef]
17. Thakur, A.; Sharma, S.; Ganjoo, R.; Assad, H.; Kumar, A. Anti-Corrosive Potential of the Sustainable Corrosion Inhibitors Based on Biomass Waste: A Review on Preceding and Perspective Research. *J. Phys. Conf. Ser.* **2022**, *2267*, 012079. [CrossRef]
18. Padhy, S.K.; Patnaik, P.; Tripathy, B.C.; Ghosh, M.K.; Bhattacharya, I.N. Electrodeposition of manganese metal from sulphate solutions in the presence of sodium octyl sulphate. *Hydrometallurgy* **2016**, *165*, 73–80. [CrossRef]
19. Padhy, S.K.; Tripathy, B.C.; Alfantazi, A. Effect of Sas additives on electrodeposition manganese metal (Emm) from sulfate solutions in the presence of sodium metabisulphite. *Hydrometallurgy* **2018**, *177*, 227–236. [CrossRef]
20. Xue, J.R.; Wang, S.; Zhong, H.; Li, C.X.; Wu, F.F. Influence of sodium oleate on manganese electrodeposition in sulfate solution. *Hydrometallurgy* **2016**, *160* (Suppl. C), 115–122. [CrossRef]
21. Fan, X.; Xi, S.Y.; Sun, D.G.; Liu, Z.H.; Du, J.; Tao, C.Y. Mn–Se interactions at the cathode interface during the electrolytic-manganese process. *Hydrometallurgy* **2012**, *127–128*, 24–29. [CrossRef]
22. Etxebarria, N.; Arana, G.; Antolin, R.; Borge, G.; Posata, T.; Raposa, J.C. Selenium in electrolytic manganese as a reference material for the quality control of aluminium melts. *Accred. Qual. Assur.* **2007**, *12*, 575–580. [CrossRef]
23. Zhao, L.Y.; Siu, A.C.; Leung, K.T. Anomalous electrodeposition of metallic Mn nanostructured films on H-terminated Si(100) at anodic potential. *Chem. Mater.* **2007**, *19*, 6414–6420. [CrossRef]
24. Sharma, R.K.; Rastogi, A.C.; Singh, G. Electrochemical growth and characterization of Manganese telluride thin films. *Mater. Chem. Phys.* **2004**, *84*, 46–51. [CrossRef]
25. Griskonis, E.; Sulcius, A.; Zmuidzinaviciene, N. Influence of temperature on the properties of Mn coatings electrodeposited from the electrolyte containing Te(VI) additive. *J. Appl. Electrochem.* **2014**, *44*, 1117–1125. [CrossRef]
26. Galvanauskaite, N.; Sulcius, A.; Griskonis, E.; Diaz-Arista, P. Influence of Te(VI) additive on manganese electrodeposition at room temperature and coating properties. *Trans. IMF* **2011**, *89*, 325–332. [CrossRef]
27. Kondratas, D.Z.; Stulpinas, B.B.; Petroshevichyute, O.S. Corrosion properties of selenium-containing manganese galvanic deposits alloyed with iron subgroup metals. Scientific works of universities Lit. SSR. *Chem. Chem. Technol.* **1976**, *18*, 164–170.
28. Li, W.P.; Zuo, X.L.; Liang, J.H.; He, J.H.; Zhang, S.T. Effect of acetate on electrodeposition of manganese from chloride electrolyte with SeO_2 additives. *Adv. Mater. Res.* **2014**, *937*, 193–199. [CrossRef]
29. Galvan-Reyes, C.; Fuentes-Aceituno, J.C.; Salinas-Rodríguez, A. The role of alkalizing agent on the manganese phosphating of a high strength steel part 1: The individual effect of NaOH and NH4OH. *Surf. Coat. Technol.* **2016**, *291*, 179–188. [CrossRef]
30. Hosseini, M.R.; Sarabi, A.A.; Mohammadloo, E.E.; Sarayloo, M. The performance improvement of Zr conversion coating through Mn incorporation: With and without organic coating. *Surf. Coat. Technol.* **2016**, *258*, 437–446. [CrossRef]
31. Duszczyk, J.; Siuzdak, K.; Klimczuk, T.; Strychalska-Nowak, J.; Zaleska-Medynska, A. Manganese Phosphatizing Coatings: The Effects of Preparation Conditions on Surface Properties. *Materials* **2018**, *11*, 2585. [CrossRef] [PubMed]
32. Alvarado-Macías, G.; Fuentes-Aceituno, J.C.; Rodríguez, A.S.; Rodríguez-Varela, F.J. Understanding the Nature of the Manganese Hot Dip Phosphatizing Process of Steel. *J. Mex. Chem. Soc.* **2013**, *57*, 328–336. [CrossRef]

33. Yingsamphancharoen, T.; Srisuwan, N.; Rodchanarowan, A. The electrochemical investigation of the corrosion rates of welde pipe ASTM A106 Grade B. *Metals* **2016**, *6*, 207. [CrossRef]
34. Available online: https://matweb.com/search/datasheet.aspx?matguid=67e1b53cedc944b19ae5a9d46cef3096&ckck=1 (accessed on 12 June 2023).
35. *EN ISO 9227:2022*; Corrosion Tests in Artificial Atmospheres. Salt Spray Tests. ISO: Geneva, Switzerland, 2022; p. 18.
36. Singh, K.; Rani, N. Study of role of phosphate coating properties electrophoretic paint performance by EIS and simulated corrosion tests. *Trans. IMF* **2014**, *92*, 153–160. [CrossRef]
37. Crozier, B.M.; Liu, Q.; Ivey, D. Electrodeposition of an iron–cobalt phase isostructural to α-Mn. *ECS Trans.* **2009**, *16*, 141–154. [CrossRef]

Disclaimer/Publisher's Note: The statements, opinions and data contained in all publications are solely those of the individual author(s) and contributor(s) and not of MDPI and/or the editor(s). MDPI and/or the editor(s) disclaim responsibility for any injury to people or property resulting from any ideas, methods, instructions or products referred to in the content.